Biosensors Hot Paper

DOI: 10.1002/ange.201404720

Chemical Vapor Detection Using a Reconstituted Insect Olfactory Receptor Complex**

*Koji Sato and Shoji Takeuchi**

Abstract: *The sensing of vapor odorants is highly demanded in the field of life and medical sciences. Although olfactory receptors (ORs) have potentials to recognize volatile organic compounds, the interaction of ORs, chemical vapors, and peptide components in olfactory mucus has yet to be analyzed to develop OR-based sensors. A bioinspired electrophysiology technique is shown to record the response of reconstituted insect ORs to chemical vapors. To mimic the interface between ORs and olfactory mucus, OR expressing spheroids were loaded into a hydrogel microchamber array. A negative extracellular field potential shift of spheroids was successfully observed by the stimulation of their vapor cognate ligand. Importantly, the ligand repertoire of the OR of malaria vector mosquito examined by this method differed from that of in vivo studies. Our method is useful to develop protein-based gas sensing techniques and to examine the binding of ORs and chemical vapors.*

The olfactory receptor (OR) gene family encodes the most sophisticated protein-based chemical-sensing elements found in nature. Individual animals possesses approximately 100 (insect) to 1000 (rodent) functional OR proteins that each recognize a multiple of cognitive ligands in an overlapping manner in their ligand repertoire.[1] In the process of olfactory perception, vapor odorant molecules first diffuse into the thin layer of olfactory mucus or lymph covering the surface of peripheral olfactory receptor neurons. The odorants then diffuse to and bind to ORs located on the surface of OR neurons, resulting in the activation of electrical neural events that transmit signals to the higher nervous system. Because OR ligands include biomedical markers and environmental factors, considerable effort has been expended to develop bioengineered OR-based artificial noses for biomedical applications, environment sensing, and biochemical research.[2–5] In particular, OR-based biosensors using functional OR expression platforms provide powerful tools for the screening of volatile organic compounds and identification of their receptors.

OR-based biosensors require that extracellular domains of OR proteins should be maintained in aqueous buffer solution to stabilize the dynamic interaction between seven-transmembrane domains of ORs and phospholipids. Therefore, previous olfactory systems using reconstituted ORs were capable of detecting only chemicals dissolved in aqueous solution. Techniques for vapor olfactory stimulation of heterologous OR-expressing cells have not been developed, and thus the fundamental question as to whether air-phase compounds are capable of activating reconstituted OR proteins remains to be answered. Here, we describe an electrophysiological technique using an OR-based vapor phase olfactory sensor for measuring the olfactory responsiveness of OR-expressing mammalian cells to chemical vapors. We integrated the spheroids of OR-expressing human embryonic kidney cells (HEK293T) into a hydrogel microchamber system designed to mimic the olfactory gas-liquid interface and protect the cells from the external environment to prevent drying.

Figure 1 shows the concept of insect OR-expressing HEK293T spheroids and the principle behind their electrical response to odorants. Because insect ORs consist of odor-gated ion channels that convert odorant chemical information into cation currents independent of G-protein signaling pathways (Figure 1b),[6–8] the system does not require the co-expression of any G-protein subunits or downstream ion channels to produce electrical events.[9] Moreover, ORs are the molecular basis of host-seeking and feeding behaviors of pathogen vector insects, many of which constitute populations that must be controlled to protect public health. HEK cells are the most frequently used cells to reconstitute the functional OR proteins.[1,6,7,9] Their spheroid formation by using microfluidic techniques has also been reported.[10] Because the current conductance of a single OR ion channel complex is 20 pS at resting cell membrane potential,[6] spheroid formation might also be efficient to amplify the small current conductance by the cell assembly.

The surface of OR neurons is covered by olfactory mucus in vertebrates and by lymph in insects. This covering ranges between approximately 0.5 and 5 μm in thickness and acts to keep the epithelial cells moist.[11] In the vertebrate nose, mucus is secreted from the Bowman's gland.[12] To mimic this

[*] Dr. K. Sato, Prof. S. Takeuchi
Institute of Industrial Science, The University of Tokyo
4-6-1 Komaba, Meguro-ku, Tokyo (Japan)
and
ERATO Takeuchi Biohybrid Innovation Project, JST
Komaba Open Laboratory, 4-6-1 Komaba, Meguro-ku, Tokyo (Japan)
E-mail: takeuchi@iis.u-tokyo.ac.jp
Prof. S. Takeuchi
Institute of Industrial Science, The University of Tokyo
4-6-1 Komaba, Meguro-ku, Tokyo (Japan)

[**] This work was supported by the JST (Japan Science and Technology Agency). We thank M. Onuki and M. Kato-Negishi (The University of Tokyo) for helping in the fabrication of PDMS molds. We also thank A. Hsiao for useful comments on this manuscript. K. Sato also was supported in part by grants from the Ministry of Education, Culture, Sports, Science and Technology of Japan (Grant-in-Aid for Scientific Research Young Scientist (A), grant number 21680035; Grant-in-Aid for Basic Research (C), grant number 26390036).

Supporting information for this article is available on the WWW under http://dx.doi.org/10.1002/anie.201404720.

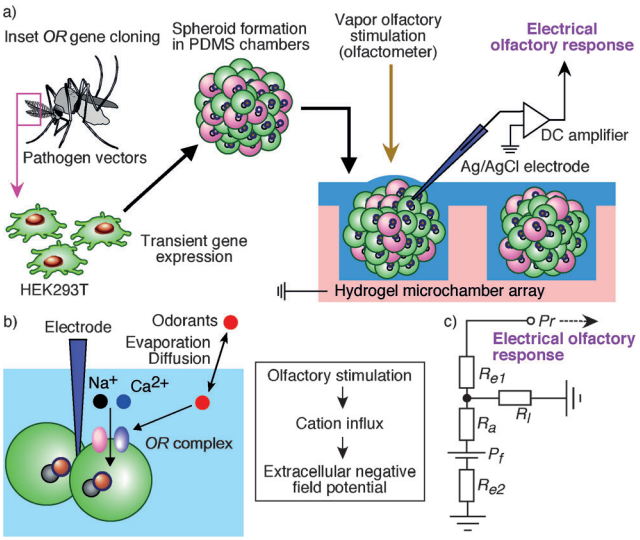

Figure 1. An extracellular field potential recording of the olfactory response of OR-expressing spheroids to vapor-phase odorant stimulation. a) Experimental procedure. Insect odor-gated ion channels were transiently expressed in HEK293T cells. The cells were then dispersed into the wells of PDMS microchambers to form spheroids. OR-expressing spheroids were loaded onto the surface of a hydrogel microchamber, and the extracellular field potential of the individual spheroid was recorded. Vapor olfactory stimulation was performed using an olfactometer. b) Principle of extracellular field potential shift evoked by odorants. c) Equivalent-circuit model of the extracellular field potential recording. R_{e1}, R_{e2}, R_l, R_a, P_f, and P_r represent the recording electrode resistance, grand electrode resistance, leak resistance, access resistance, real field potential, and recorded field potential, respectively.

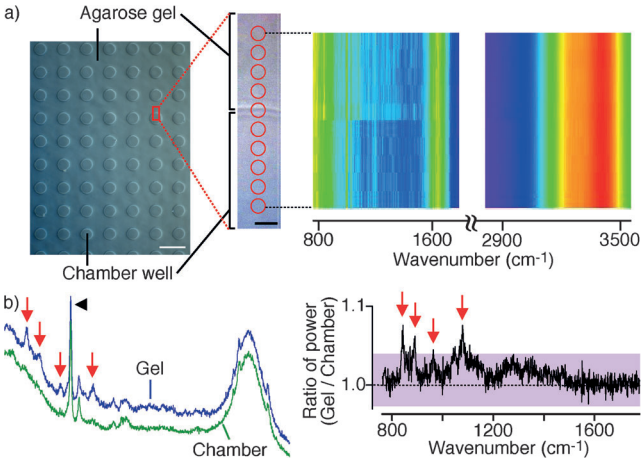

Figure 2. Laser Raman scattering spectra of the agarose microchamber. a) Macroscopic image of microchambers (left) and pseudo-colored Raman spectra (right) acquired by the surface scanning of the hydrogel chamber (red circles, middle). Red and blue pseudo-colors correspond to the maximal and minimal intensity, respectively. White bar = 200 μm; black bar = 10 μm. b) Averaged Raman scattering spectra collected at gel (blue) or chamber well (green) region ($n = 5$ each) and ratios of their power (right). Shaded regions around the black trace represent the background power distribution calculated from the C–O–C bonds independent power spectra (1150–1800 cm^{-1}). Red arrows indicate peaks of C–O–C bonds, and the black arrowhead indicates C–C bonds.

source of mucus, we constructed a hydrogel microchamber composed of the extracellular buffer solution including 1.5% agarose (*w*/*v*; Figure 2). Using confocal laser Raman microscopy, we observed Raman scattering associated with O–H bonds (ca. 3400 cm^{-1}) originating from the surface of the hydrogel chamber well, indicating the presence of buffer solution in the microchambers (Figure 2a). Four 800–1150 cm^{-1} peaks assigned to the agarose gel specific C–O–C bonds were detected from the region of hydrogel,[13] whereas these peaks were not observed in analyses of the chamber well (Figure 2b). Around the 800–1150 cm^{-1} wavenumber region, the strongest peak at 1000 cm^{-1} originated from C–C bonds was detected from both hydrogel and chamber well regions. As expected, Raman scattering of O–H bonds associated with the chamber well was detected for more than 1 h. Thus, the buffer solution used for spheroid electrophysiology analyses was maintained in the hydrogel chamber.

In olfactory organs, chemical compounds in the vapor phase dissolve in the mucus or lymph and then reach ORs. Because of technical difficulties associated with controlling the surface aqueous layer and the gas-liquid interface, the processes involved in vapor odorant diffusion and interaction with ORs has yet to be observed using heterologous functional expression systems. Thus, the comparison of olfactory responsiveness of reconstituted ORs to chemical vapors and that of in vivo studies has not yet been examined. To address this issue and develop OR-based chemical vapor sensors, we assessed the capability of OR expressing spheroids to detect the chemical vapors of their cognate ligands.

Insect OR-expressing HEK293T cells were prepared using a conventional chemical-based transfection technique.[6,9] To assemble the ORs and prevent adhesion, which could interfere with the spatial cell arrangement in physiological experiments, HEK293T spheroids were formed by culturing transfected cells in a polydimethylsiloxane (PDMS) microchamber array.[14] The spheroids were then loaded into the wells of an agarose-based hydrogel chamber array to record the extracellular field potential. Vapor olfactory stimulation was achieved using a conventional olfactometer.[15] This integrated system was employed to maintain wet conditions and protect the cells from desiccation during vapor olfactory stimulation.

At first, we prepared four plasmids for the functional expression of insect OR complexes in mammalian cell lines. We expressed the malaria vector mosquito (*Anopheles gambiae*) protein GPROR2, a receptor for 2-methylphenol (2-MP), and the fruitfly (*Drosophila melanogaster*) protein Or47a, a receptor for pentyl acetate (PA).[2,16] When these ORs are expressed in mammalian cell lines such as HEK293T together with an olfactory co-receptor (Orco: AgOrco for *A. gambiae*, Orco for *D. melanogaster*), the cells show influx of extracellular calcium and cation-nonselective ion conductance upon stimulation with their cognate ligands. To visualize OR proteins, we expressed DsRed:OR N-terminus fusion proteins in HEK293T cells (Figure S1). As previously reported,[2,6,8,16] using the aqueous buffer exchange system, we confirmed that intracellular calcium increases in OR

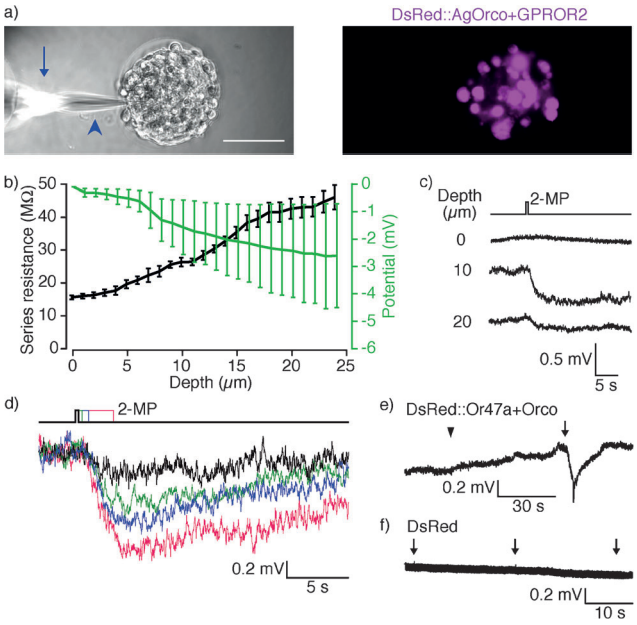

Figure 3. The characteristics of insect OR-expressing HEK293T spheroids and their olfactory responses. a) Images of an *A. gambiae* OR (GPROR2 + DsRed:AgOrco, magenta)-expressing HEK293T spheroid loaded into an agarose microchamber and its field potential recording. The arrowhead and arrow indicate the recording electrode and the surface of the buffer solution, respectively. White bar = 100 μm. b) Series resistance (left Y-axis and black trace) and basal extracellular field potential (right Y-axis and green trace) along the depth of spheroids. c, d) Extracellular field potential recordings of a spheroid expressing GPROR2 + DsRed:AgOrco and stimulated with the headspace of 1 mM 2-methyl phenol (2-MP) solution, with various electrode depth recording positions (c) and durations of 2-MP stimulation (d). e) Extracellular field potential recordings of a spheroid expressing *Drosophila* ORs (DsRed:Or47a + Orco) and stimulated with the headspace of 4 mM pentyl acetate (PA) solution (arrow) or background air (arrowhead) for 1 s. f) Extracellular field potential recordings of a spheroid expressing DsRed and stimulated with the headspace of 1 mM 2-MP solution for 0.5 s (arrows). Data are shown as mean ± SD ($n = 5$).

complex-expressing cells upon stimulation with their cognate ligand.

To verify the olfactory responsiveness of insect OR-expressing HEK293T spheroids, we recorded the extracellular field potential of spheroids upon vapor olfactory stimulation (Figure 3). For the electrophysiology recordings, we loaded the OR-expressing spheroids into the hydrogel chamber well (Figure 3a). Because the gas–liquid interface was visible at the edge of the glass electrode, the thickness of the extracellular buffer solution was estimated at 10–200 μm. Figure 1c shows the equivalent-circuit model of an extracellular field potential recording of a spheroid. In this circuit, the extracellular field potential (P_r) and series resistance (R_s) are described by Equations (1) and (2):

$$P_r = P_f R_l/(R_a + R_l) \quad (1)$$

$$R_s = R_{e1} + R_l(R_a + R_{e2})/(R_l + R_a + R_{e2}) \quad (2)$$

where R_{e1}, R_{e2}, R_l, R_a, and P_f denote the recording electrode resistance, grand electrode resistance, leak resistance, access resistance, and real field potential, respectively. R_{e1}, R_{e2}, and R_a are constants determined by the experimental condition of each electrodes and medium buffer solutions, whereas R_l depends on the position of the tip of electrode. From Equation (1), it is evident that a high leak resistance is necessary to avoid a voltage drop in the field potential. From Equation (2), we can see that the increasing leak resistance increases the series resistance resulting in improvement of the extracellular field potential recording.

In the extracellular field potential recording, the detection of the intrinsic negatively charged potential of cell surface is the essential step to confirm that the electrode appropriately contacts with the target cells or tissues.[15] To examine how the recording condition changes during the electrode insertion to the HEK293T spheroids, we measured the spontaneous basal field potential and corresponding the series resistance at different depth (Figure 3b). The negative charge was not recorded from the surface of spheroids (0 μm), indicating the extracellular potential cannot be measured at this position; this is probably due to the low series resistance compared with the electrode resistance. As the electrode was inserted deeper into the spheroid, the series resistance increased, whereas the field potential of the inner spheroid shifted to negative. As HEK293T cells are about 10–20 μm in size, a depth of approximately 20 μm corresponded to the boundary between the surface and inner layers of the cell. Because vapor chemicals would stimulate mostly the outer layer cells, we speculated that odor-induced extracellular field potential response would be recordable at the depth of 10–20 μm.

To examine the effect of vapor olfactory stimulation on the extracellular field potential and optimize the recording position of electrode tip depth, we stimulated GPROR2 + DsRed:AgOrco-expressing spheroids with the headspace of 1 mM 2-MP solution and recorded the extracellular field potential at various electrode tip depths (Figure 3c). A negative field potential shift following olfactory stimulation was observed at a depth of 10 μm. The magnitude of the response decreased at a depth of 20 μm. The ratio of response magnitude recorded at depth of 20 μm to 10 μm was 0.32 ± 0.31 (mean ± SD, $n = 3$). Because the background white noise was not affected by the depth, the data indicated that the optimal electrode depth was 10 μm. Under these conditions, shifts in the extracellular field potential of insect OR-expressing HEK293T spheroids following chemical vapor stimulation could be recorded.

To examine the response kinetics of the GPROR2 + AgOrco-expressing spheroids, we recorded the extracellular field potential at various durations of 2-MP stimulation (Figure 3d). The latency of GPROR2 + AgOrco-mediated field potential responses (1037 ± 220 ms, mean ± SD, $n = 7$) (Figure S2) was 50 times larger than that of previously reported whole-cell current responses.[6] The delay in response onset was probably due to the rate of diffusion, because the layer of extracellular buffer solution in this experiment was thicker than what would be expected in vivo (Figure 3a). Similar to the results of intracellular calcium imaging analyses of GPROR2 + AgOrco-expressing cells,[6] the rising phase of the 2-MP-induced electrical response was not modulated by the duration of stimulation. This result

suggests that the electrical response is derived from activation of the insect OR complexes by 2-MP diffusing from the vapor phase.

We also expressed the *Drosophila* Or47a + Orco receptor complex and control DsRed alone in HEK293T spheroids (Figure 3e,f). DsRed:Or47a + Orco-expressing HEK293T spheroids showed no response to background air stimulation, but a negative shift in the extracellular field potential was observed upon stimulation with the head space of 4 mM PA solution. No shift in the extracellular field potential of DsRed-expressing HEK293T spheroids was observed upon stimulation with the headspace of 1 mM 2-MP solution. These data suggest that our method enables the quantitative measurement of insect OR activity, or alternatively, the detection of their ligands diffused from chemical vapors.

Figure 4 shows an example of a continuous recording of the olfactory responsiveness of a GPROR2 + AgOrco-expressing spheroid. The extracellular field potential following stimulation with the headspace of 1 mM 2-MP solution was monitored for 30 minutes. The insect olfactory organ is a powerful biosensor and is frequently used to screen for semiochemical compounds that control behavior and reproductive status.[2,4,17] The electrical activity of olfactory receptor neurons can be monitored using continuous air-flow of gas chromatography (GC)-fractionated biosamples (i.e., the GC-electroantennographic detection [GC-EAD] method).[17] The recording stability of our technique indicates that OR-expressing mammalian cell lines may be applicable to the screening of olfactory biomarkers fractionated by GC.

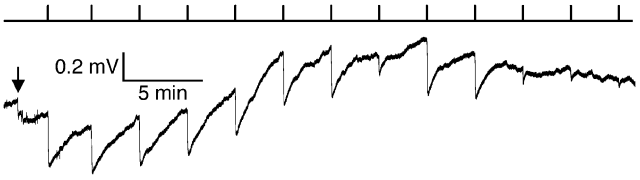

Figure 4. Continuous extracellular field potential recordings of a spheroid expressing GPROR2 + AgOrco and stimulated with the headspace of 1 mM 2-MP for 0.5 s. An arrow indicates the timing of electrode insertion into the spheroid. Top trace indicates the timing of olfactory stimulation.

The greatest advantage of our method is that it can be used to examine the binding affinity of reconstituted ORs and chemical vapor ligands. In rodents, odorant specificity and sensitivity differ between genetically identified olfactory receptor neurons in vivo, isolated olfactory receptor neurons from the olfactory epithelium, and heterologous OR-expressing cell lines.[18,19] Several studies have demonstrated OR-independent modification of olfactory coding in vivo.[19,20] It was thought that this phenomenon is not crucial for the identification of ligand-OR pairing in insects.[21] However, the GPROR2 + AgOrco complex, which was identified as a 2-MP receptor using an in vivo ectopic OR-expression system,[2] responds to both 2-MP and benzaldehyde (BA) in heterologous OR-expressing HEK293T cells[6] and *Xenopus* oocytes.[22] Because the ligands are delivered using a solution exchanging system in both heterologous functional expression systems, we hypothesized that vapor and aqueous phase differences between the olfactory stimulation systems affect the ligand selectivity of ORs in heterologous OR-expressing cells. To test this hypothesis, we examined the response of reconstituted GPROR2 + AgOrco-expressing HEK293T spheroids to 2-MP and BA in the vapor phase at various biologically relevant concentrations.

In calcium imaging experiments using the aqueous olfactory stimulation system, GPROR2 + AgOrco-expressing HEK293T cells showed similar dose-dependent intracellular calcium responses to both aqueous 2-MP and BA (Figure 5b,d), similar to previous reports.[6,22] However, the reconstituted OR showed a significantly greater response to vapor-phase BA than 2-MP in our system (Figure 5c,e). These results demonstrate that both the heterologous expression system and olfactory stimulation method affect the ligand repertoire of insect ORs. Because the reconstituted OR responded to both 2-MP and BA, the lower sensitivity to 2-MP was thought to be due to limited diffusion of vapor-phase 2-MP into the buffer solution rather than due to differences in the molecular structure of the OR complex in different phospholipid bilayer cell membranes. The water solubility and vapor pressure of 2-MP (2.5 g/100 mL and 0.033 kPa, respectively) and BA (0.33 g/100 mL and 0.133 kPa) suggest that vapor pressure rather than water solubility is a greater determinant of vapor olfactory responsiveness. Nonetheless, measurements of melting rates of ligands under the experimental condition would be necessary to clarify our hypothesis. However, the mechanism in GPROR2-expressing antennae that enhances the response to 2-MP and diminishes the response to BA in vivo is unclear. It is thought that both

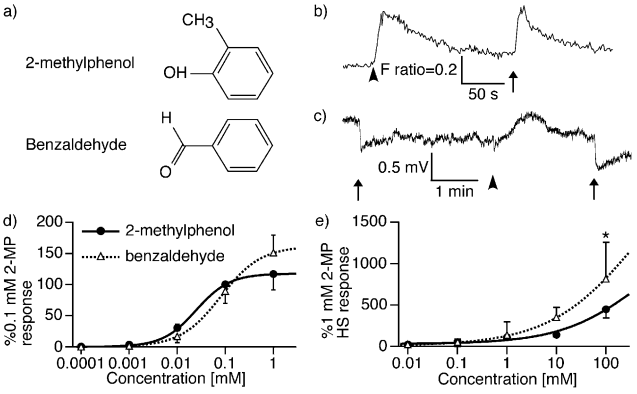

Figure 5. Dose-dependent responses of GPROR2 + AgOrco OR complexes to 2-MP and benzaldehyde (BA) determined using various olfactory stimulation methods. a) The structures of the odorants used in this experiment. b,d) Responses of ORs to aqueous olfactory stimulation were examined using calcium imaging. c,e) Responses of ORs to vapor olfactory stimulation were examined using the method described in this study. b,c) Response examples. The arrowhead and arrow indicate the timing of 2-MP and BA stimulation, respectively. d,e) Dose response curves for each olfactory stimulation method. Odorant responses are shown as a percentage of the response to 0.1 mM 2-MP (d) or the headspace (HS) of 1 mM 2-MP solution (e) and are fitted to the Hill equation (mean ± SD, $n = 5$). Significance assessed by *U*-test: $*p < 0.05$.

selective transport of hydrophilic odorants by a family of odorant-binding proteins[23] and enzymatic degradation of odorants[19] in the olfactory mucus and lymph modulate olfactory discrimination at the peripheral level.

In summary, we describe here a method integrating cell assembly and heterologous gene expression techniques to enable recording of the electrophysiology of insect OR-expressing cells stimulated with chemical vapors. We were able to observe the olfactory response of ORs to known ligands, demonstrating the high efficiency and reliability of our methodology as an OR-based olfactory sensor. Although the reconstituted ORs responded to vapor olfactory stimulation at biologically relevant concentrations, their ligand repertoire in in vivo recording with vapor olfactory stimulation differed from that of heterologous OR-expressing cells with vapor olfactory stimulation. Taken together, these data suggest that the compounds in mucus surrounding the surface of olfactory receptor neurons affect the olfactory recognition mechanism. Our methodology would be applicable to the functional analysis of the role of peptide components in olfactory mucosa and to the development of ligand-activated ion channel-based biosensors.

Received: April 26, 2014
Published online: July 28, 2014

Keywords: biosensors · ion channels · olfaction · receptors

[1] K. Touhara, L. B. Vosshall, *Annu. Rev. Physiol.* **2009**, *71*, 307 – 332.
[2] E. A. Hallem, A. N. Fox, L. J. Zwiebel, J. R. Carlson, *Nature* **2004**, *427*, 212 – 213.
[3] a) J. Minic, M. A. Persuy, E. Godel, J. Aioun, I. Connerton, R. Salesse, E. Pajot-Augy, *FEBS J.* **2005**, *272*, 524 – 537; b) Q. Liu, H. Cai, Y. Xu, Y. Li, R. Li, P. Wang, *Biosens. Bioelectron.* **2006**, *22*, 318 – 322; c) V. Radhika, T. Proikas-Cezanne, M. Jayaraman, D. Onesime, J. H. Ha, D. N. Dhanasekaran, *Nat. Chem. Biol.* **2007**, *3*, 325 – 330; d) C. Wu, P. Chen, H. Yu, Q. Liu, X. Zong, H. Cai, P. Wang, *Biosens. Bioelectron.* **2009**, *24*, 1498 – 1502; e) E. H. Oh, H. S. Song, T. H. Park, *Enzyme Microb. Technol.* **2011**, *48*, 427 – 437.
[4] S. Nojima, C. Schal, F. X. Webster, R. G. Santangelo, W. L. Roelofs, *Science* **2005**, *307*, 1104 – 1106.
[5] N. Misawa, H. Mitsuno, R. Kanzaki, S. Takeuchi, *Proc. Natl. Acad. Sci. USA* **2010**, *107*, 15340 – 15344.
[6] K. Sato, M. Pellegrino, T. Nakagawa, T. Nakagawa, L. B. Vosshall, K. Touhara, *Nature* **2008**, *452*, 1002 – 1006.
[7] D. Wicher, R. Schäfer, R. Bauernfeind, M. C. Stensmyr, R. Heller, S. H. Heinemann, B. S. Hansson, *Nature* **2008**, *452*, 1007 – 1011.
[8] T. Nakagawa, M. Pellegrino, K. Sato, L. B. Vosshall, K. Touhara, *PLoS One* **2012**, *7*, e32372.
[9] S. Katada, T. Nakagawa, H. Kataoka, K. Touhara, *Biochem. Biophys. Res. Commun.* **2003**, *305*, 964 – 969.
[10] K. Lee, C. Kim, J. Young Yang, H. Lee, B. Ahn, L. Xu, J. Yoon Kang, K. W. Oh, *Biomicrofluidics* **2012**, *6*, 114114 – 141147.
[11] J. V. Fahy, B. F. Dickey, *N. Engl. J. Med.* **2010**, *363*, 2233 – 2247.
[12] E. Houtmeyers, R. Gosselink, G. Gayan-Ramirez, M. Decramer, *Eur. Respir. J.* **1999**, *13*, 1177 – 1188.
[13] H. Onoe, T. Okitsu, A. Itou, M. Kato-Negishi, R. Gojo, D. Kiriya, K. Sato, S. Miura, S. Iwanaga, K. Kuribayashi-Shigetomi, Y. T. Matsunaga, Y. Shimoyama, S. Takeuchi, *Nat. Mater.* **2013**, *12*, 584 – 590.
[14] M. Kato-Negishi, Y. Tsuda, H. Onoe, S. Takeuchi, *Biomaterials* **2010**, *31*, 8939 – 8945.
[15] K. D. Cygnar, A. B. Stephan, H. Zhao, *J. Vis. Exp.* **2010**, *2*, DOI: 10.3791/1850.
[16] A. A. Dobritsa, W. van der Goes van Naters, C. G. Warr, R. A. Steinbrecht, J. R. Carlson, *Neuron* **2003**, *37*, 827 – 841.
[17] D. L. Struble, H. Arn in *Techniques in Pheromone Research* (Eds.: H. E. Hummel, T. A. Miller), Springer, New York, **1984**, pp. 161 – 178.
[18] Y. Oka, S. Katada, M. Omura, M. Suwa, Y. Yoshihara, K. Touhara, *Neuron* **2006**, *52*, 857 – 869.
[19] A. Nagashima, K. Touhara, *J. Neurosci.* **2010**, *30*, 16391 – 16398.
[20] R. L. Doty, E. L. Cameron, *Physiol. Behav.* **2009**, *97*, 213 – 228.
[21] a) A. F. Carey, G. Wang, C. Y. Su, I. J. Zwiebel, J. R. Carlson, *Nature* **2010**, *464*, 66 – 71; b) F. Scialò, B. S. Hansson, E. Giordano, C. L. Polito, F. A. Digilio, *PLoS One* **2012**, *7*, e36538.
[22] G. Wang, A. F. Carey, J. R. Carlson, L. J. Zwiebel, *Proc. Natl. Acad. Sci. USA* **2010**, *107*, 4418 – 4423.
[23] F. F. Damberger, E. Michel, Y. Ishida, W. S. Leal, K. Wührich, *Proc. Natl. Acad. Sci. USA* **2013**, *110*, 18680 – 18685.